

Spinal cord reconstitution with homologous neural grafts enables robust corticospinal regeneration

Ken Kadoya^{1,2}, Paul Lu^{1,3}, Kenny Nguyen¹, Corinne Lee-Kubli¹, Hiromi Kumamaru¹, Lin Yao^{4–6}, Joshua Knackert^{4–6}, Gunnar Poplawski¹, Jennifer N Dulin¹, Hans Strobl¹, Yoshio Takashima¹, Jeremy Biane¹, James Conner¹, Su-Chun Zhang⁴ & Mark H Tuszynski^{1,3}

The corticospinal tract (CST) is the most important motor system in humans, yet robust regeneration of this projection after spinal cord injury (SCI) has not been accomplished. In murine models of SCI, we report robust corticospinal axon regeneration, functional synapse formation and improved skilled forelimb function after grafting multipotent neural progenitor cells into sites of SCI. Corticospinal regeneration requires grafts to be driven toward caudalized (spinal cord), rather than rostralized, fates. Fully mature caudalized neural grafts also support corticospinal regeneration. Moreover, corticospinal axons can emerge from neural grafts and regenerate beyond the lesion, a process that is potentially related to the attenuation of the glial scar. Rat corticospinal axons also regenerate into human donor grafts of caudal spinal cord identity. Collectively, these findings indicate that spinal cord ‘replacement’ with homologous neural stem cells enables robust regeneration of the corticospinal projection within and beyond spinal cord lesion sites, achieving a major unmet goal of SCI research and offering new possibilities for clinical translation.

Despite recent progress in promoting the regeneration of many classes of central nervous system axons after SCI, the corticospinal projection remains largely refractory to regeneration^{1,2}. Yet the CST, which arises from the cerebral cortex and projects to the spinal cord, is the most important projection for voluntary movement in humans, and its failure to regenerate has been a major limiting factor in the advancement of potential regenerative therapies to humans. Previous reports indicate that corticospinal axons spared from injury can sprout after SCI in mice, rats and nonhuman primates^{3–5}, and that tissue spared by incomplete SCI can facilitate the growth of some injured corticospinal axons^{6,7}. However, efforts to elicit true corticospinal axon regeneration—growth of the transected axon into a spinal cord lesion cavity—have met with very limited success. For example, although early-life knock-down of the phosphatase and tensin homolog (*PTEN*) promotes the growth of adult corticospinal axons across a small lesion gap⁸, this effort fails in larger lesions that lack spared astrocyte bridges⁸, and it is less effective when applied after injury^{9,10}. Similarly, many studies that target myelin-associated inhibitory Nogo receptors report modest growth or the sprouting of corticospinal axons, but fall well short of promoting extensive regeneration into the lesion sites themselves^{6,11}. Finally, although overexpression of tropomyosin receptor kinase B (*TrkB*) enables corticospinal axons to regenerate into a cell graft placed at a subcortical lesion site¹², this same strategy does not accomplish regeneration into a more distantly located spinal cord lesion site¹².

The failure of corticospinal axons to regenerate after SCI stands in stark contrast to the success of the experimentally induced regeneration

of other descending motor systems, including the reticulospinal^{13–15}, raphespinal^{13–16} and propriospinal^{14,16} projections. Neural stem cells and neural progenitor cells (NPCs) have the potential to reconstitute lesion sites with neurons and glia^{17–20}. Furthermore, they can replace lost adult neural tissue with cells that are homologous to those in the pre-injured state, either by driving them to specific regional fates^{21,22} or by isolating NPCs from homologous regions of the developing nervous system²³. We now report that homologous reconstitution of the lesioned adult spinal cord with caudalized neural stem cells or with primary spinal cord–derived NPCs supports the robust regeneration of corticospinal axons, which form functional excitatory synapses with the neural replacement graft.

RESULTS

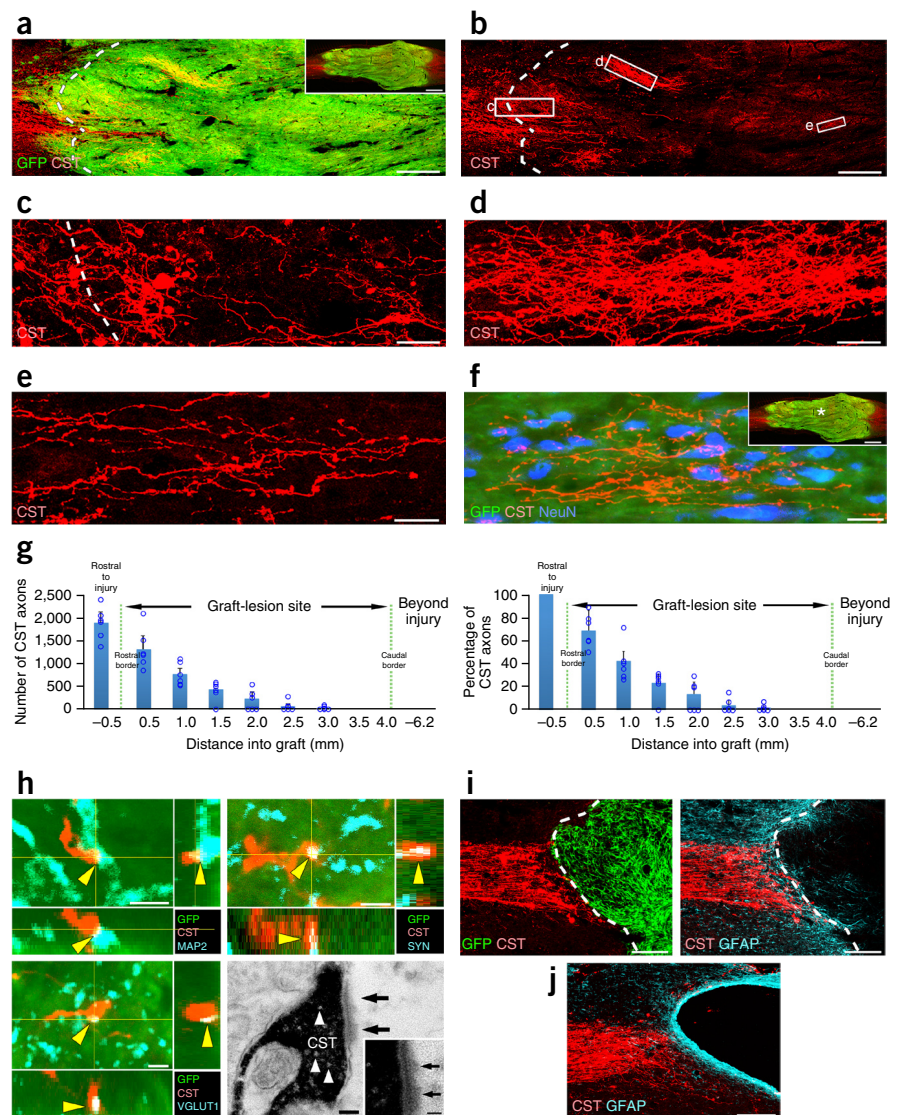
Corticospinal axons extensively regenerate into NPC grafts

We grafted GFP-expressing, multipotent NPCs derived from embryonic day 14 (E14)-rat spinal cord primordia (see Online Methods) into injury sites in six adult female Fischer 344 rats 2 weeks after complete transection at T3. Analysis of anterogradely labeled corticospinal axons 6 weeks after grafting revealed extensive regeneration of this projection into the grafts (Fig. 1a–f). A mean of $1,650 \pm 310$ corticospinal axons was quantified at a distance of 0.5 mm within the graft (Fig. 1g, left), representing 63% of all corticospinal axons quantified 0.5 mm rostral to the lesion site (Fig. 1g, right). Corticospinal axons regenerating into NPC grafts contacted dendrites of grafted cells that were labeled for microtubule-associated protein 2 (MAP2) (Fig. 1h). Many of these

¹Department of Neurosciences, University of California, San Diego, La Jolla, California, USA. ²Department of Orthopaedic Surgery, Hokkaido University, Sapporo, Japan. ³Veterans Administration San Diego Healthcare System, San Diego, California, USA. ⁴Waisman Center, University of Wisconsin–Madison, Wisconsin, USA. ⁵Department of Neuroscience, University of Wisconsin–Madison, Wisconsin, USA. ⁶Department of Neurology, University of Wisconsin–Madison, Wisconsin, USA. Correspondence should be addressed to M.H.T. (mtuszynski@ucsd.edu).

Received 19 March 2015; accepted 12 February 2016; published online 28 March 2016; doi:10.1038/nm.4066

Figure 1 Corticospinal axons extensively regenerate into NPC grafts. **(a,b)** Rostral aspect of a GFP-expressing, multipotent NPC graft in the site of T3 complete spinal cord transection, shown in horizontal section. Left, rostral; right, caudal. CST axons are labeled with biotinylated dextran amine (BDA, red). Inset shows overview of the graft. Dashed line indicates host-graft interface in **a–c**. Scale bar, 240 μm ; 1 mm (inset). **(b)** Same field as **a**; the CST approaches and regenerates into an NPC graft in the lesion site. Scale bar, 240 μm . **(c–e)** Higher-magnification views of boxed areas in **b** show the density, varicosities and tortuosities of regenerating corticospinal axons that extend into the graft. Scale bars, 60 μm (**c**); 30 μm (**d**); 20 μm (**e**). **(f)** Regenerating CST axons surround neurons in the center of the graft (asterisk, inset), 3 mm from the rostral host-graft border. Inset, overview of the graft. Scale bar, 20 μm ; 1 mm (inset). **(g)** Left, quantification of CST axons in NPC grafts in six rats. Right, quantification of the proportion of CST axons in NPC grafts, normalized to the total number of CST axons 0.5 mm rostral to the lesion site in six rats. Data are presented as mean \pm s.e.m. Circles indicate data from individual rats. **(h)** Triple labeling for GFP, CST and MAP2 demonstrates a CST axon in the graft that exhibits a bouton-like swelling in close apposition to a dendrite of a grafted neuron, labeled with MAP2 (arrowheads; upper left; scale bar, 2 μm). Triple labeling for GFP, CST and synaptophysin (SYN; upper right; scale bar, 2 μm) or VGLUT1 (lower left; scale bar, 2 μm) in the graft. Yellow arrowheads indicate co-localization of CST axon terminals with SYN and VGLUT1 (arrowheads). Electron-microscopy image of a 3,3'-diaminobenzidine (DAB)-labeled CST axon terminal (black) forming a synapse (black arrows) with a neuronal process within the graft (lower right). Scale bar, 50 nm. White arrowheads indicate presynaptic vesicles. Scale bar inset, 100 nm. **(i)** Sagittal images of GFP-expressing syngenic bone marrow stromal cell (MSC) grafts in the site of C4 spinal cord transection. Left, double labeling for CST axons (red) and GFP-expressing MSCs (green); right, double labeling for CST axons and GFAP (blue). Dashed lines indicate rostral host-graft interface. Scale bars, 200 μm . **(j)** Sagittal image of CST axons in a C4-CST transection lesion in the absence of any graft. Scale bar, 200 μm .



contacts exhibited bouton-like morphology (**Fig. 1h**) and co-localized with the presynaptic marker synaptophysin (**Fig. 1h**) and with vesicular glutamate transporter 1 (VGLUT1; **Fig. 1h**; glutamate is the appropriate neurotransmitter for corticospinal axons)²⁴. Synapse formation through the regeneration of corticospinal axons into NPC grafts was confirmed by electron microscopy (**Fig. 1h**). By contrast, lesioned control groups that either received grafts of syngenic bone marrow stromal cells (MSCs) or that did not receive any grafts exhibited no corticospinal-axon regeneration into the lesion site (**Fig. 1i,j** and **Supplementary Fig. 1**). Cell grafts that included either Schwann cells or MSCs secreting either brain-derived neurotrophic factor (BDNF) or neurotrophin 3 (NT-3) also failed to support corticospinal regeneration into lesion sites (**Supplementary Fig. 1**).

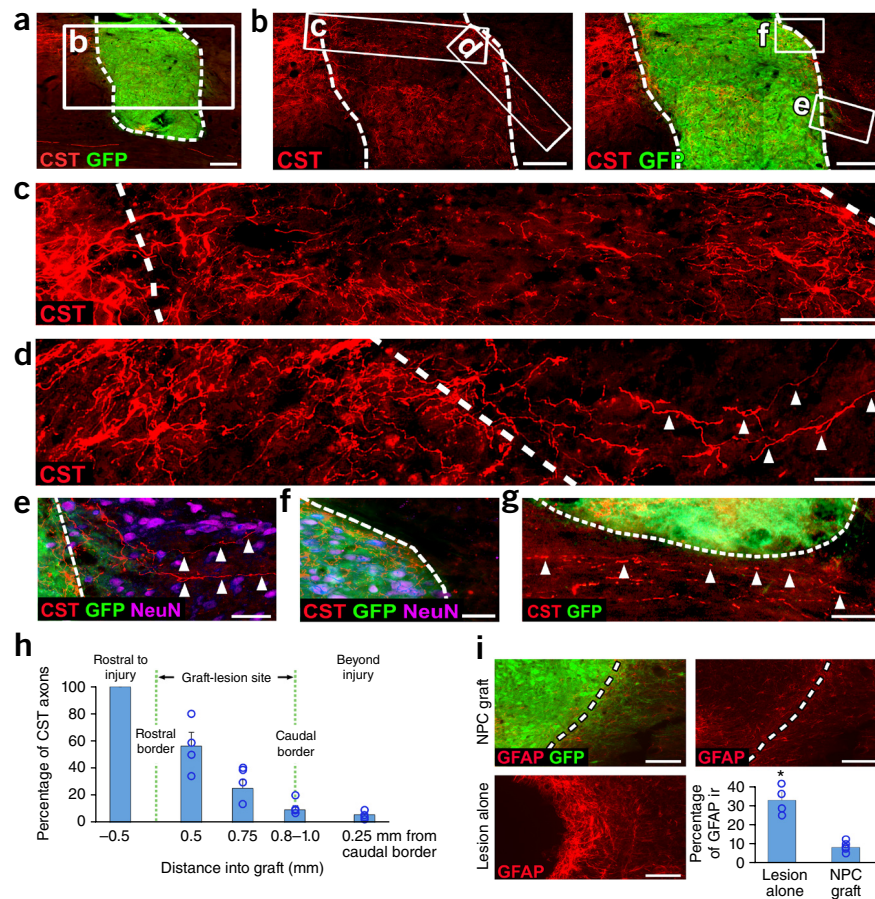
Corticospinal axons can regenerate beyond lesion sites

In the T3-transection model, corticospinal axons grew for a maximum distance of 2.5–3.0 mm into grafts placed at the lesion site (**Fig. 1g**). To determine whether corticospinal axons could regenerate beyond

the lesion site if a small lesion and graft were placed, we performed focal CST lesions without resecting the lateral and ventral portions of the spinal cord in an effort to limit the rostral-to-caudal length of the lesion cavity and graft. E14 NPCs were placed into this small lesion by using a graft cell volume of 1.5 μl (3×10^5 cells) ($n = 6$ rats), instead of the 10 μl (2×10^6 cells) used in the above studies. When examined 6 weeks after grafting, four of six animals had small grafts and lesions of ~ 1.0 mm rostral-to-caudal length, as compared to the 2.5–3.0 mm length observed in those above. In all four of these animals, corticospinal axons crossed the caudal graft-host interface, indicative of regeneration beyond the lesion site (**Fig. 2a–d**). An average of 9.7% of all corticospinal axons quantified at 0.5 mm rostral to the lesion site crossed the caudal host-graft interface into gray matter but not into white matter (**Fig. 2e–h**).

It is possible that axons crossing the caudal graft-host interface could have arisen from spared ventral or lateral corticospinal axons that were actually entering the graft from the caudal direction, rather than exiting the graft from the rostral direction. However, we did not

Figure 2 Axonal regeneration beyond the graft in focal CST lesions. **(a)** Low-magnification sagittal overview of CST axons (red) and an E14-rat spinal cord NPC graft (green), placed at the focal CST lesion site 6 weeks after injury. Scale bar, 200 μ m. Dashed lines indicate the host-graft interface throughout. Rostral is to the left throughout. **(b)** High-magnification views of boxed area in **a**. Scale bars, 200 μ m. **(c)** High-magnification view of boxed area in **b** (left), including rostral host-graft interface. Scale bar, 100 μ m. **(d)** High-magnification view of boxed area in **b** (left). Arrowheads indicate CST axons extending beyond the caudal host-graft interface. Scale bar, 50 μ m. **(e–g)** High-magnification views of the boxed areas in **b** (right). **(e)** Arrowheads indicate CST axons penetrating host gray matter (NeuN-positive) but not white matter (**f**, NeuN-negative) caudal to the graft-lesion site. Scale bars, 50 μ m (**e**); 100 μ m (**f**). **(g)** High-magnification view of the area just ventral to the graft-lesion site. Arrowheads indicate spared ventral CST axons located close to the NPC graft. Scale bar, 50 μ m. **(h)** Quantification of the proportion of regenerating CST axons found at different locations across the rostro-caudal axis of the NPC graft ($n = 4$ rats). **(i)** Example images of GFAP immunoreactivity (ir) in the vicinity of the host-graft interface of focal CST-lesioned rats after receiving (top) or not receiving (lower left) NPC graft. Scale bars, 100 μ m. Quantification of GFAP ir at the lesion boundary (lower right; $n = 4$ rats, lesion alone; $n = 4$ rats, NPC graft). Circles indicate data from individual rats. * $P < 0.05$; Wilcoxon test. Error bars represent mean \pm s.e.m. for all panels.



observe corticospinal axons crossing the caudal graft-host interface in animals that had partial lesions but larger grafts of 2.5–3.0 mm, thereby counteracting this possibility (Fig. 3–c). Moreover, careful analysis of spared ventral corticospinal axons in very close proximity to the graft demonstrated no instances of axonal penetration into the graft (Fig. 2g), whereas lesioned dorsal corticospinal axons clearly crossed the host-lesion interface to penetrate the graft (Figs. 1a–c and 2c). Labeling for glial fibrillary acidic protein (GFAP) revealed a significant attenuation of the reactive glial scar surrounding the lesion-graft site ($P < 0.05$; Fig. 2i).

Single-synapse anatomical relays span the lesion

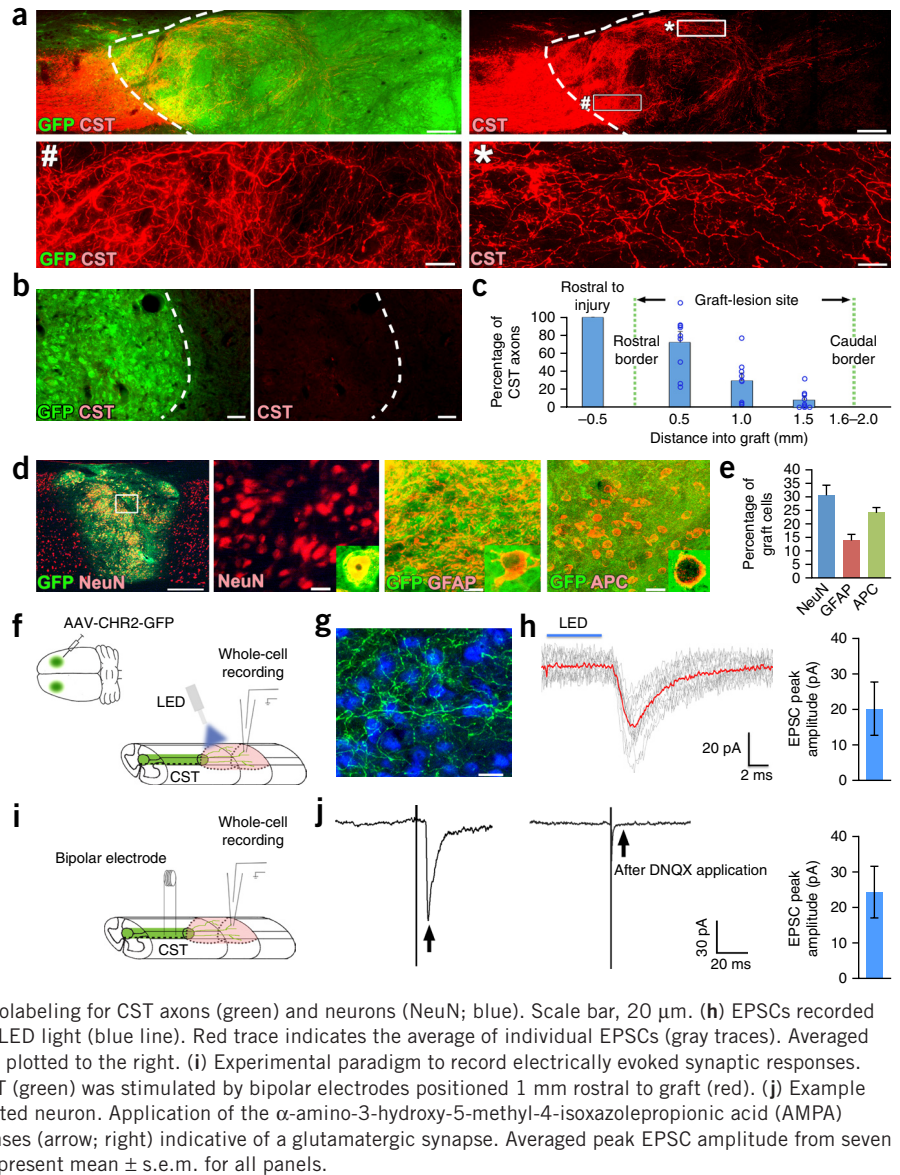
Next, to determine whether regenerating corticospinal axons form connections with grafted neurons that in turn directly project axons to the spinal cord caudal to the lesion site, we injected the retrograde tracer cholera toxin B (CTB) into spinal cord gray matter that was located two spinal cord segments caudal to the lesion-NPC graft site of four rats, 6 weeks after C4-CST lesions and NPC grafts (Supplementary Fig. 2a–c). When examined 3 d after CTB injections, retrogradely labeled grafted neurons exhibited close appositions with BDA-labeled corticospinal axons in every rat examined (Supplementary Fig. 2d–f). Corticospinal axon terminals on these grafted, retrogradely labeled neurons expressed VGLUT1 (Supplementary Fig. 2g). Quantification revealed that 1.8% of grafted neurons had been retrogradely labeled with CTB; 26% of these received BDA-labeled corticospinal axon appositions, and 92% of those grafted neurons expressed the excitatory neuronal marker CAMK2 (Supplementary Fig. 2h,i).

Regenerating corticospinal axons form functional synapses with grafted neurons

Having established that corticospinal axons regenerate extensively into NPC grafts, we performed additional experiments to further characterize the regenerating axons and to identify the cellular mechanisms associated with regeneration. For these studies, we used C4-CST lesions in either rat or mouse species; in rats, the CST is located in the dorsal columns and contains >98% of all corticospinal axons⁵. The chief advantage of this lesion model, which is less extensive than complete transection, is that animal care is less difficult, and the grafts survive and fill the lesion cavity without the need for a growth-factor cocktail¹⁹ (Fig. 3a), which thereby eliminates potentially confounding effects of growth factors that complicate the interpretation of mechanisms underlying corticospinal regeneration. Nine rats received implants of E14-derived, multipotent NPC grafts (2.5 μ l; 5×10^5 cells) into the C4-CST lesion cavities at the same time that the lesions were made. When examined 6 weeks later, surviving grafts had filled the lesion site and had supported robust corticospinal regeneration: the number of corticospinal axons that were quantified at a distance of 0.5 mm within the graft represented 72% of the total number of corticospinal axons quantified 0.5 mm rostral to the lesion (Fig. 3c). The NPC grafts expressed mature neuronal, glial and oligodendrocyte markers (Fig. 3d,e), as had been observed in the T3 complete-transection model¹⁹.

To assess whether the synapses formed between regenerating corticospinal axons and neurons in the lesion site (Fig. 1h) were functional, we injected adeno-associated virus 2 (AAV2) vectors expressing channelrhodopsin-2 (CHR2) and GFP into the motor

Figure 3 Electrophysiological connectivity between regenerating corticospinal axons and grafted neurons. **(a)** Sagittal views of CST axons (red) and GFP-expressing NPC grafts (green) placed in C4-CST lesions in rats 6 weeks after injury. Dashed lines in **a** indicate rostral host-graft border. Rostral is to the left throughout. Bottom images (#,*) are high-magnification views of boxed areas at upper right. Scale bars, 200 μm (top); 50 μm (bottom). **(b)** Sagittal views of the caudal graft-host interface (dashed lines) in a C4 CST-lesioned rat, depicting CST axons (red) and GFP-expressing NPC grafts (green). Scale bars, 50 μm . **(c)** Quantification of the proportion of regenerating CST axons (normalized to the total number of CST axons 0.5 mm rostral to the graft-lesion site) found at different locations across the rostro-caudal axis of the NPC graft ($n = 9$ rats). Circles indicate data from individual rats. **(d)** Double immunolabeling of GFP-labeled NPC grafts (green) with neuronal (NeuN; red), astrocytic (GFAP; red) and mature oligodendrocytic (adenomatous polyposis coli, APC; red) cell-type markers. Boxed region in the low-magnification image on the left is shown at higher magnification immediately to the right. Scale bars, 500 μm (left); 20 μm (three images on right). **(e)** Quantification of cell-type marker immunoreactivity in grafts. NeuN, blue; GFAP, red; APC, green. **(f)** Experimental paradigm to record optogenetically evoked synaptic responses. AAV2 vectors expressing CHR2 and GFP were injected into motor cortices (green), followed by NPCs grafts into lesion cavities 2 weeks later. Four weeks after NPC grafts, CHR2+ CST axons were stimulated with blue LED light ($n = 3$ rats), and whole-cell recordings of grafted neurons were performed. CST axons, green; graft, red; LED light, blue. **(g)** Double immunolabeling for CST axons (green) and neurons (NeuN; blue). Scale bar, 20 μm . **(h)** EPSCs recorded from a grafted neuron evoked with 5 ms of 470-nm LED light (blue line). Red trace indicates the average of individual EPSCs (gray traces). Averaged peak EPSC amplitude from three responding cells is plotted to the right. **(i)** Experimental paradigm to record electrically evoked synaptic responses. During whole-cell recordings of grafted neurons, CST (green) was stimulated by bipolar electrodes positioned 1 mm rostral to graft (red). **(j)** Example of an evoked EPSC (arrow; left) recorded from a grafted neuron. Application of the α -amino-3-hydroxy-5-methyl-4-isoxazolepropionic acid (AMPA) receptor antagonist DNQX (20 μM) abolished responses (arrow; right) indicative of a glutamatergic synapse. Averaged peak EPSC amplitude from seven responding cells is plotted to the right. Error bars represent mean \pm s.e.m. for all panels.



cortex of three adult rats. Two weeks after AAV2 injections, E14-rat multipotent NPC grafts were placed into C4-CST lesion sites at the time of injury (**Fig. 3f,g**). Four weeks after injury and grafting, spinal cord slices were prepared for whole-cell recording of optogenetically evoked synaptic responses in the grafted neurons. Photostimulation generated excitatory postsynaptic currents (EPSCs) in three out of 14 graft neurons sampled from two of the rats (**Fig. 3h**), and the EPSCs were abolished in the presence of the glutamatergic blocker 6,7-dinitroquinoxaline-2,3-dione (DNQX; 20 μM). The presence of functional excitatory synapses was confirmed with a second method, wherein we placed bipolar stimulating electrodes in the main dorsal CST at a position 1 mm rostral to the lesion, and we performed whole-cell recording in graft neurons (**Fig. 3i**). EPSCs were detected in seven out of 14 graft neurons sampled from three rats (**Fig. 3j**). These responses were abolished in the presence of DNQX (20 μM), which confirmed that the responses were the result of glutamatergic synaptic activation and not a consequence of antidromic activation of graft axons within the host tissue or of current spread reaching the grafted cells.

Corticospinal regeneration requires an injury signal and contact with the graft

As prior studies have indicated that axotomy primes peripheral neurons for regeneration^{25,26}, we next examined whether an injury signal was required for corticospinal regeneration. We placed NPC grafts immediately dorsal to and in contact with the CST at the C4 level in 12 rats, without transecting the corticospinal projection. Six of these animals then received CST lesions at the C5 level, one segment caudal to the graft, whereas the other six rats underwent sham surgeries that did not include CST lesions (**Fig. 4a,b**). When assessed 6 weeks later, corticospinal axon regeneration into grafts was observed only in those animals with transections of the CST (**Fig. 4c-g**).

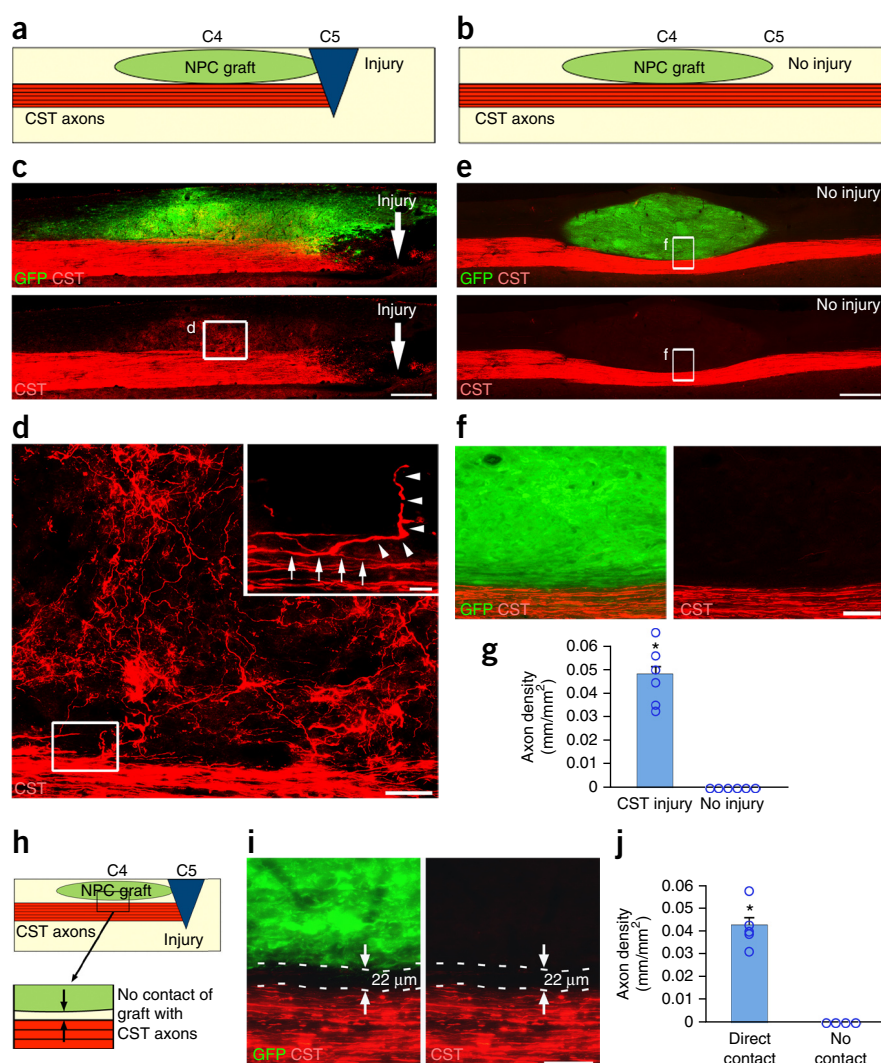
To investigate whether regeneration is contact mediated or generated by diffusible factors from the graft, we performed C5-CST lesions in rats and, at the same time, placed NPC grafts immediately dorsal to the corticospinal projection at a position one segment rostral to the C4 level. Grafts were placed either in contact with the CST ($n = 5$) or more superficially, within 22–50 μm of the tract but not in actual contact with corticospinal axons in the tract ($n = 4$; **Fig. 4h**).

Figure 4 Corticospinal regeneration requires an injury signal and contact with neural grafts. **(a,b)** Experimental design to determine whether an injury signal is required to enable CST axon regeneration. NPC grafts were placed into the spinal sensory columns at the C4 level immediately dorsal to the CST. In injured animals **(a)**, a spinal cord lesion was placed at C5, transecting the dorsal corticospinal projection. 'No-injury' animals did not receive a lesion **(b)**. **(c–f)** Low- and high-magnification views of BDA-labeled CST axons (red) with GFP-expressing NPC graft (green) in the presence of **(c,d)** or in the absence of **(e,f)** CST injury. Rostral is left; caudal is right. Scale bars, 500 μm **(c,e)**; 50 μm **(d)**; 100 μm **(f)**. **(d)** High-magnification views of boxed area in **(c)** depict a corticospinal axon in the main tract (arrows, inset) that gives off a branch (arrowheads, inset), which penetrates the graft (inset; scale bar, 10 μm). **(f)** High-magnification of boxed areas in **(e)**, shown with (left) or without (right) inclusion of the GFP channel. **(g)** Quantification of CST axon regeneration into grafts with or without C5 injury. $*P < 0.01$, Wilcoxon test. **(h)** Experimental design to determine the requirement of physical contact between the NPC graft and injured CST axons. NPCs are grafted to C4, and a spinal cord injury is placed at C5 (as in **a**), but in some cases with a 22–50- μm gap (between black arrows) interposed between the graft and the CST. **(i)** High-magnification views of a 22- μm gap between NPC graft and injured CST axons. Scale bar, 50 μm . **(j)** Quantification of CST axons in grafts with or without direct contact of grafts with CST. $*P < 0.01$, Wilcoxon test. For all panels, error bars represent mean \pm s.e.m., and circles indicate data from individual rats.

When examined 6 weeks later, corticospinal axons had regenerated into every graft that had contact with the tract, but not into any grafts located even the short distance of 22–50 μm from the tract (**Fig. 4i,j**).

Mature grafts support corticospinal regeneration

We hypothesized that only early-stage NPC grafts would enable corticospinal regeneration, given that molecules for axon guidance, patterning and differentiation are expressed during the developmental stages of the nervous system and that the mature spinal cord is generally considered to be nonpermissive to axonal regeneration²⁷. To assess whether the developmental stage of NPCs influences corticospinal regeneration, we first characterized the time course of maturation of E14 spinal cord-derived NPCs after grafting into the C4 spinal cord *in vivo* (in the absence of spinal cord lesions), and we sacrificed rats 7, 20 and 70 d later ($n = 3$ rats per time point). We found that grafted NPCs predominantly expressed the developmental markers nestin (NPCs) and doublecortin (DCX, immature neurons) 1 week after grafting (**Supplementary Fig. 3a**). A mix of early (nestin; DCX) and mature neuronal markers (NeuN) were evident 20 d after grafting, and mature markers (neuronal NeuN and oligodendrocyte adenomatous polyposis coli, APC) were exclusively expressed 70 d after grafting (a time point equivalent to the age of a mature rat; **Supplementary Fig. 3a**). To assess whether axons can regenerate into mature neural grafts, we took advantage of the observation that corticospinal axons initiate a regeneration signal only when injured. Accordingly,



we grafted E14 spinal cord-derived NPCs immediately dorsal to and in contact with the intact CST at C4, and allowed the grafts to mature for 0, 20 or 70 d. C5–CST lesions were then performed at each of these time points ($n = 5$ rats with lesions performed the same day; $n = 4$ rats with lesions at 20 d and $n = 6$ rats with lesions 70 d after grafting; **Supplementary Fig. 3b**). Our analysis of corticospinal regeneration into grafts, assessed 6 weeks after the rats received lesions, revealed that fully mature grafts supported regeneration equally robust to that supported by immature grafts (**Supplementary Fig. 3c–e**).

Corticospinal regeneration requires caudalized, homotypic neuronal grafts

Next, we hypothesized that replacement of the spinal cord lesion site with homologous neural tissue would be required to support corticospinal regeneration. Accordingly, NPC grafts were prepared from either the spinal cord, hindbrain or telencephalon of E14 rats and grafted into adult C4–CST lesions ($n = 9$ recipients of spinal cord grafts; $n = 7$ of hindbrain; $n = 7$ of telencephalic grafts). We found significant differences in the ability of corticospinal axons to regenerate into grafts isolated from different levels of the neuraxis, with fewer axons penetrating into grafts of the hindbrain than into those of the spinal cord, and with corticospinal axons largely failing to penetrate telencephalic grafts (Kruskal-Wallis test, $P < 0.01$; **Fig. 5a,b**).

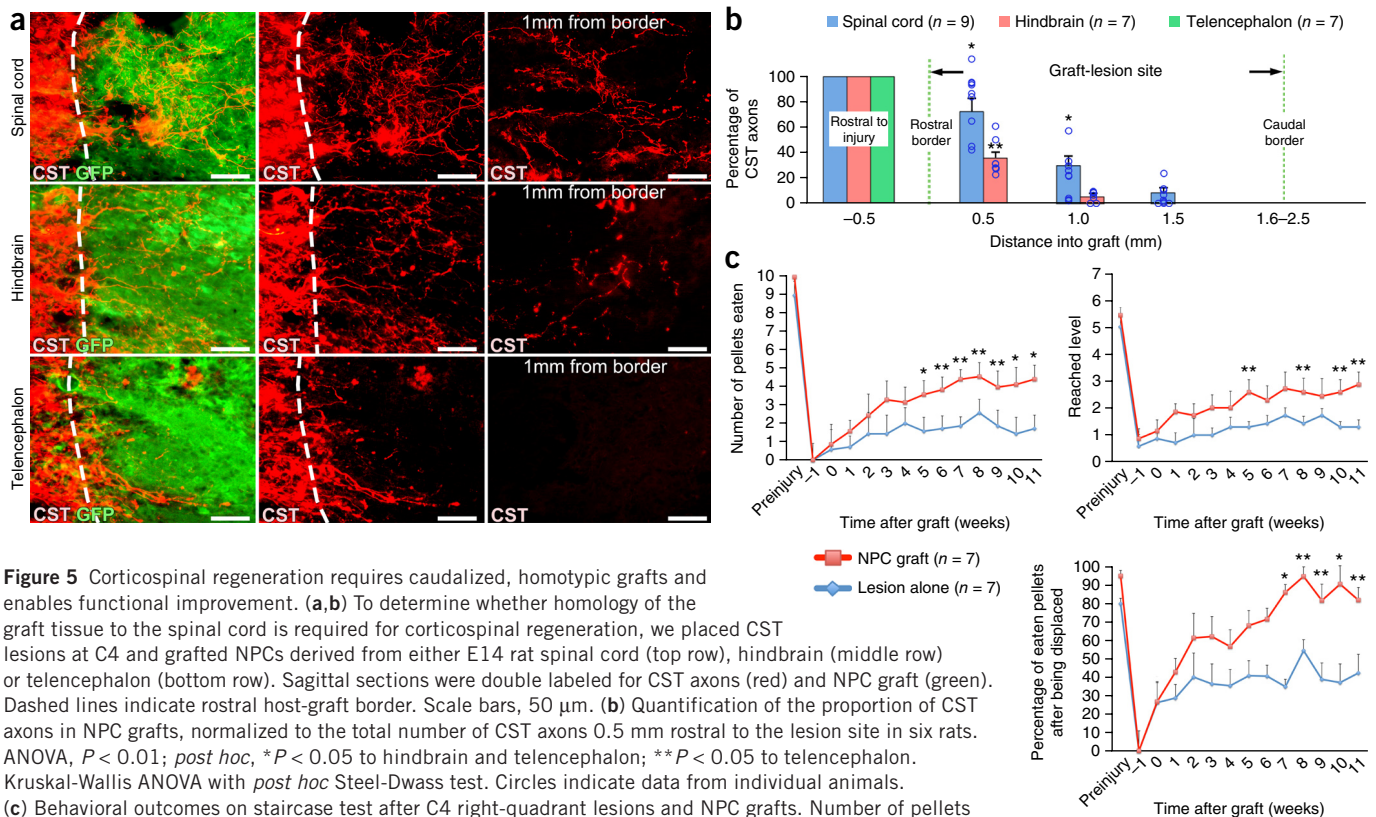


Figure 5 Corticospinal regeneration requires caudalized, homotypic grafts and enables functional improvement. **(a,b)** To determine whether homology of the graft tissue to the spinal cord is required for corticospinal regeneration, we placed CST lesions at C4 and grafted NPCs derived from either E14 rat spinal cord (top row), hindbrain (middle row) or telencephalon (bottom row). Sagittal sections were double labeled for CST axons (red) and NPC graft (green). Dashed lines indicate rostral host-graft border. Scale bars, 50 μ m. **(b)** Quantification of the proportion of CST axons in NPC grafts, normalized to the total number of CST axons 0.5 mm rostral to the lesion site in six rats. ANOVA, $P < 0.01$; *post hoc*, $*P < 0.05$ to hindbrain and telencephalon; $**P < 0.05$ to telencephalon. Kruskal-Wallis ANOVA with *post hoc* Steel-Dwass test. Circles indicate data from individual animals. **(c)** Behavioral outcomes on staircase test after C4 right-quadrant lesions and NPC grafts. Number of pellets eaten (upper left); repeated-measures ANOVA, $P < 0.05$ with *post hoc* Fischer's on individual days indicated by asterisks; $*P < 0.01$; $**P < 0.05$. Maximum depth of staircase reached (upper right) and pellet-grasping accuracy (lower right), repeated-measures ANOVA, $P = 0.07$ on both tasks; exploratory *post hoc* Fischer's shown with $*P < 0.01$; $**P < 0.05$. Error bars represent mean \pm s.e.m. for all panels.

The greatest degree of regeneration among these graft types occurred into grafts of NPCs derived from the spinal cord ($P < 0.05$, *post hoc* Steel-Dwass test, as compared to hindbrain; $P < 0.01$ as compared to telencephalon).

To test the hypothesis that neurons are an essential component of the graft to enable corticospinal regeneration, we prepared neuronal-restricted progenitor cells (NRPs) and glial-restricted progenitor cells (GRPs) from the developing E12-mouse spinal cord²⁸. For this study, we used mice instead of rats because we failed to achieve survival of rat NRPs in lesion sites, as reported in previous studies²⁹. Adult mice underwent C4-CST lesions and received implants of either GRPs alone ($n = 9$), a mixture of NRPs and GRPs ($n = 4$) or E12-mouse multipotent NPCs ($n = 9$; **Supplementary Fig. 4a–c**). When examined 6 weeks later, grafts of GRPs alone failed to support corticospinal axon regeneration (**Supplementary Fig. 4c,d**). However, grafts containing a mixture of NRPs and GRPs had surviving neurons and glia, and supported the same degree of corticospinal regeneration as the grafts of E12-mouse multipotent NPCs (**Supplementary Fig. 4c,d**).

NPC grafts improve forelimb function after SCI

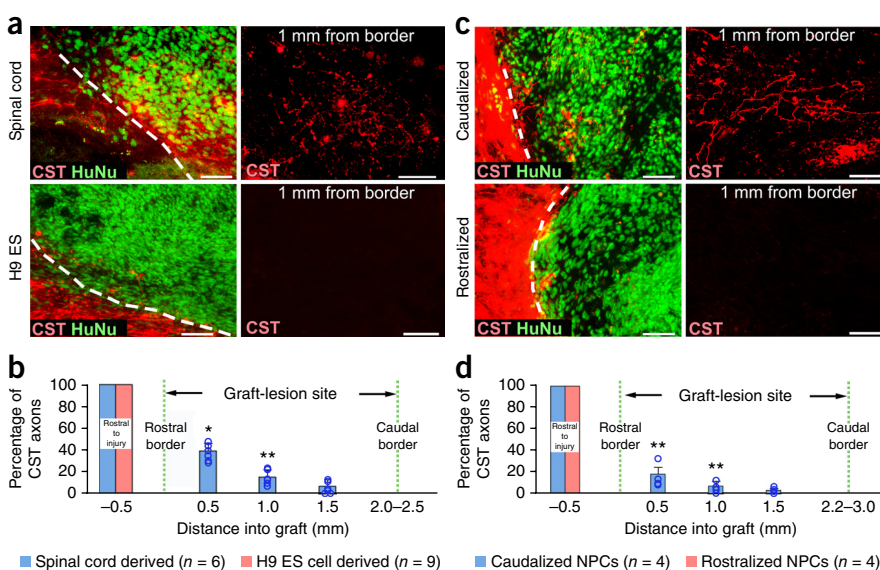
To determine whether NPC grafts influence functional recovery, we performed behavioral assessments in rats using a skilled forelimb reaching task (the staircase task³⁰), which is dependent on the motor cortex^{31–34} and reflects in part the function of the corticospinal projection^{5,30,35}. For this portion of the study, we used bilateral CST lesions as well as right dorsal-quadrant lesions of the spinal cord, which removed the ipsilateral rubrospinal and lateral corticospinal projections (**Supplementary Fig. 5a,b**)^{36,37}. Adult rats were pre-operatively trained and lesioned, and then randomly assigned

to either receive grafts 2 weeks later of syngeneic E14 rat-derived multipotent NPCs ($n = 9$) or to have their lesion site re-exposed without grafting ($n = 9$; **Supplementary Fig. 5a–c**). One control subject died 1 week after sham surgery. Two animals were excluded from final analysis because of poor graft survival (**Supplementary Fig. 5g,h**), and one control animal was excluded because of an incomplete lesion that spared the CST. After lesions but before grafting, all animals exhibited a severe loss of function on the staircase task (**Fig. 5c**). After grafting, the treatment group exhibited statistically superior performance compared to control lesioned subjects in overall food pellet-retrieval success with the affected forelimb (repeated-measures analysis of variance (ANOVA), $P < 0.05$; *post hoc* Fischer's showed significant differences on specific testing days between the grafted and lesioned groups beginning 5 weeks after grafting; **Fig. 5c**). Repeated-measures ANOVA carried out on two other functional submeasures of skilled forelimb performance on the staircase task also approached the significance threshold, including the animals' performance results on the most difficult level of the staircase reached ($P = 0.07$) and the percentage of displaced pellets that were eaten ($P = 0.07$). Given the presence and consistency of these trends, we performed exploratory *post hoc* analyses that yielded findings consistent with total pellet retrieval: the treatment group performed better than the lesion control group on specific testing days from about 5 weeks after grafting (**Fig. 5c**).

NPCs do not migrate when grafted into closed lesion cavities

Recent reports indicate that NPCs grafted into open lesion cavities can form ectopic cell colonies^{38–41}. This presents a safety concern for clinical trials. Among the animals in this study, we comprehensively

Figure 6 Homotypic human NPC grafts support corticospinal regeneration. **(a)** Sagittal views of human NPC grafts derived from either spinal cord (top row) or the H9 ES cell line, driven toward a rostral midbrain fate (bottom row) placed at C4-CST injury in immunodeficient rats. Graft cells are labeled with human nuclear marker (HuNu; green) and CST axons are BDA labeled (red). **(b)** Quantification of proportion of CST axons in NPC grafts, normalized to total number of CST axons 0.5 mm rostral to lesion site. $n = 6$ rats; spinal cord–derived grafts. $n = 9$ rats; H9 ESC–derived grafts. Wilcoxon test, $*P < 0.01$; $**P < 0.05$. **(c)** Sagittal views of human NPC grafts comprising either caudalized (hindbrain; top row) or rostralized (forebrain; bottom row) NPCs derived from human iPSCs placed in C4-CST lesion sites in immunodeficient rats. **(d)** Quantification of the proportion of CST axons in NPC grafts, normalized to the total number of CST axons 0.5 mm rostral to the lesion site. $n = 4$ rats each for caudalized or rostralized iPSC-derived grafts. Wilcoxon test, $**P < 0.05$. For all panels, rostral is left; dashed lines indicate rostral host-graft border. Scale bars, 50 μm for all images. Error bars represent mean \pm s.e.m., and circles indicate data from individual animals throughout.



assessed whether ectopic cell colonies were present in the neuraxis. A total of 15 rats in this study underwent ‘open’ lesions and grafts, in which the dura is opened and cells are implanted into the open lesion with a fibrin matrix and growth-factor cocktail (**Supplementary Fig. 6a**). Of these 15 animals, six had small ectopic cell deposits. Four were in animals with complete transections, and two were in animals with C4 corticospinal and dorsolateral quadrant lesions. These were small groupings of cells located within four spinal segments of the graft site, as described in previous publications (**Supplementary Fig. 6b**)^{39,40}. None of these displaced normal spinal cord tissue. We also examined whether ectopic cell deposits were present in another 78 rats and mice that underwent grafting into ‘closed’ lesion cavities, but that did not receive supplemental growth factors. None of these subjects had ectopic cell collections or cell migration within the central canal; migration into the central canal in humans would be unlikely because it is not patent in adults⁴².

Human NPC grafts support corticospinal regeneration

To further explore the clinical relevance of NPC grafting for corticospinal axon regeneration, we grafted primary human spinal cord multipotent NPCs isolated from a 9-week-old embryo (human spinal cord neural progenitor cell line UCSD1113; see Methods) into adult immunodeficient rats¹⁹ that underwent C4-CST lesions ($n = 6$). Corticospinal axons regenerated into human spinal cord–derived NPC grafts when examined 6 weeks later (**Fig. 6a,b**). We also grafted human NPCs derived from the H9 embryonic stem (ES) cell line⁴³ into immunodeficient rats using the same experimental paradigm ($n = 9$); these cells express predominantly midbrain markers but not caudal neuraxis markers (**Supplementary Fig. 7a,b**). We hypothesized that homotypic human spinal cord–derived neural progenitor grafts, but not more rostrally fated neural grafts, would promote corticospinal regeneration. Indeed, corticospinal axons successfully regenerated into spinal cord–derived human grafts and failed to regenerate into rostrally fated human H9 neural cell grafts ($P < 0.01$; **Fig. 6a,b**). The proportion of cells expressing neuronal markers did not differ between animals that received human spinal cord grafts and those that received H9 cell grafts (**Supplementary Fig. 7d**); the proportion

of cells that expressed the glial markers GFAP and NG2 at this time point 6 weeks after implantation was $<1\%$ in both graft types, because human cells require extended time for glial differentiation⁴⁴.

We then generated human induced pluripotent stem cells (iPSCs) from skin fibroblasts and drove these toward either rostral (forebrain) or caudal NPC fates without or with the caudalizing morphogen retinoic acid, respectively (**Supplementary Fig. 7a,c**). The NPCs that had differentiated from iPSCs without the caudalizing morphogen predominantly expressed forebrain neural markers, whereas retinoic acid–treated, iPSC-derived NPCs predominantly expressed caudal neural markers (**Supplementary Fig. 7a,c**). Six weeks after grafting to C4-CST lesion sites in immunodeficient rats ($n = 4$ animals per group), corticospinal axons regenerated into human caudalized NPC grafts but not into the rostralized grafts ($P < 0.05$; **Fig. 6c,d**).

DISCUSSION

Recent reports have emphasized the importance of amplifying intrinsic neuronal signaling to promote the growth of refractory corticospinal axons after SCI^{8,45}. However, these efforts have not been successful in generating extensive corticospinal regeneration into large, clinically relevant lesion sites that lack small bridges of host tissue. We now find that NPC grafts enable the extensive and consistent regeneration of corticospinal axons into sites of severe SCI. Indeed, neural grafts achieve extensive regeneration of corticospinal axons into complete spinal cord transection sites, rather than growth only through spared tissue bridges, which is an important practical milestone for their application to the vast majority of injured humans who have lesion cavitation and relatively little spared tissue⁴⁶. Successful regeneration does not require the therapeutic activation of the corticospinal neuron *per se*; provided solely with a permissive graft milieu, we show for the first time that corticospinal axons are capable of extensive regeneration into a lesion site. The observation that the regeneration of corticospinal axons requires actual contact with the graft indicates that growth is probably mediated by ligand–receptor interactions rather than by diffusible signals from the graft. This currently unknown ligand–receptor interaction is conserved across species, including humans, given that human neural stem cells support rat corticospinal regeneration.

Regenerating corticospinal axons form synapses with grafted neurons that are functional and that recapitulate the pre-injured glutamatergic phenotype of the regenerating axon. Regenerating corticospinal synapses form onto grafted neurons that predominantly express CAMK2, and some of these neurons in turn extend axons into the caudal spinal cord, thereby establishing potential relays across the lesion site. Electrophysiological measures confirm the presence of excitatory synaptic responses generated by the regenerating corticospinal axons within the graft. Corticospinal axons also exhibit an ability to regenerate beyond the lesion site and into caudal host gray matter when small (1-mm) lesions are placed. This 'bridging' regeneration is associated with the attenuation of the glial scar at the rostral and caudal host-lesion interfaces, thus identifying another potential advantage of NPC approaches for neural repair.

Notably, corticospinal regeneration occurs only when NPCs are derived from or driven toward a caudal neural fate, resembling the normal spinal cord target of corticospinal projections. Substitution of the injured spinal cord with neural anlage from other levels of the neuraxis does not support corticospinal regeneration; essentially, the replacement of the spinal cord enables corticospinal regeneration. Surprisingly, corticospinal regeneration can occur equally well into developing or fully mature grafts, indicating that it is the homotypic nature of the graft to the spinal cord, and not its state of maturity, that supports regeneration. Caudalized human NPC grafts support murine corticospinal axon regeneration, indicating conservation of cell-cell interactions across species that enable the growth of this system. The ability to reconstitute a spinal cord milieu in the lesion site by using human neural stem cells derived from ESCs or iPSCs, rather than having to depend on a supply of fresh fetal tissue grafting⁴⁷, is an important step toward achieving the practicality needed to translate this technology to humans. The precise molecular constituent(s) of the graft that enable corticospinal regeneration must still be identified; our findings point toward a graft-specific set of extracellular-matrix molecules or cell-adhesion molecules. It is also possible that a unique glial subtype exerts a permissive role in enabling corticospinal regeneration⁴⁸.

Having the means in hand to extensively regenerate the corticospinal projection provides an important tool for both future clinical development and for elucidating our understanding of the mechanisms that underlie the regeneration of what has been the most refractory axonal system crucial for human motor function. Practical issues related to clinical translation remain to be addressed, including the identification of the optimal cell type for grafting and the establishment of safe methods for cell engraftment. Recent reports indicate that ectopic stem cell colonies can form after grafting^{38–41}, although our grafts into closed lesion cavities without growth-factor cocktails were free of ectopic colonies; additional studies will aim to optimize the grafting technique to minimize the risk of cell spread. Our findings suggest that the use of caudalized neural stem cells or NPCs will be essential for supporting corticospinal regeneration in future translational efforts.

METHODS

Methods and any associated references are available in the [online version of the paper](#).

Note: Any Supplementary Information and Source Data files are available in the [online version of the paper](#).

ACKNOWLEDGMENTS

We thank L. Graham, Y. Yang, E. Boehle, J.K. Lee, M. Kim, E. Liu, R. Pope and T. Moynihan for their technical assistance; Planned Parenthood; the Rat Resource

and Research Center, University of Missouri, Columbia, Missouri, for providing GFP rats; James Thompson at the University of Wisconsin–Madison, for providing hiPSC line IMR90; K. Wewetzer, University of Freiburg, Germany, for providing 27C7 antibody; R. Darnell, the Rockefeller University, New York, for providing Hu antibody; Y. Jones for use of the electron-microscopy core facility at Cellular and Molecular Medicine, University of California, San Diego; and the Nikon Imaging Center at Hokkaido University for use of the confocal laser microscope. This work was supported by the US Veterans Administration (Gordon Mansfield Spinal Cord Injury Consortium; to M.H.T. and P.L.) the US National Institutes of Health (NS042291 to M.H.T. and GM008349 to J.K.); the Craig H. Neilsen Foundation (to K.K., H.K. and J.N.D.); the Bernard and Anne Spitzer Charitable Trust (to M.H.T.); the Dr. Miriam and Sheldon G. Adelson Medical Research Foundation (to M.H.T. and J.C.); Kobayashi Hospital Furate Research Fund (to K.K.); the Japan Society for the Promotion of Science (to H.K.); and the Busta Family and Bleser Family funds (to S.C.Z.).

AUTHOR CONTRIBUTIONS

K.K. conceived and carried out experiments, interpreted the results and wrote the manuscript. P.L. contributed to the conception of the project and performed complete-transsection experiments. K.N. and H.S. carried out experiments. C.L.-K. and J.N.D. contributed to behavior analysis. G.P. contributed to mouse experiments. H.K. contributed to the characterization of human NPCs. L.Y., J.K. and S.-C.Z. contributed to the generation of human NPCs from iPSCs. J.B., Y.T. and J.C. performed the electrophysiological analysis. M.H.T. contributed to the conception of the project and the interpretation of results, and wrote the manuscript.

COMPETING FINANCIAL INTERESTS

The authors declare no competing financial interests.

Reprints and permissions information is available online at <http://www.nature.com/reprints/index.html>.

- Liu, K., Tedeschi, A., Park, K.K. & He, Z. Neuronal intrinsic mechanisms of axon regeneration. *Annu. Rev. Neurosci.* **34**, 131–152 (2011).
- Tuszynski, M.H. & Steward, O. Concepts and methods for the study of axonal regeneration in the CNS. *Neuron* **74**, 777–791 (2012).
- Bareyre, F.M. *et al.* The injured spinal cord spontaneously forms a new intraspinal circuit in adult rats. *Nat. Neurosci.* **7**, 269–277 (2004).
- Rosenzweig, E.S. *et al.* Extensive spontaneous plasticity of corticospinal projections after primate spinal cord injury. *Nat. Neurosci.* **13**, 1505–1510 (2010).
- Weidner, N., Ner, A., Salimi, N. & Tuszynski, M.H. Spontaneous corticospinal axonal plasticity and functional recovery after adult central nervous system injury. *Proc. Natl. Acad. Sci. USA* **98**, 3513–3518 (2001).
- Schnell, L. & Schwab, M.E. Axonal regeneration in the rat spinal cord produced by an antibody against myelin-associated neurite growth inhibitors. *Nature* **343**, 269–272 (1990).
- GrandPré, T., Li, S. & Strittmatter, S.M. Nogo-66 receptor antagonist peptide promotes axonal regeneration. *Nature* **417**, 547–551 (2002).
- Liu, K. *et al.* *PTEN* deletion enhances the regenerative ability of adult corticospinal neurons. *Nat. Neurosci.* **13**, 1075–1081 (2010).
- Zukor, K. *et al.* Short hairpin RNA against *PTEN* enhances regenerative growth of corticospinal tract axons after spinal cord injury. *J. Neurosci.* **33**, 15350–15361 (2013).
- Ohtake, Y. *et al.* The effect of systemic *PTEN* antagonist peptides on axon growth and functional recovery after spinal cord injury. *Biomaterials* **35**, 4610–4626 (2014).
- Starkey, M.L. & Schwab, M.E. Anti-Nogo-A and training: can one plus one equal three? *Exp. Neurol.* **235**, 53–61 (2012).
- Hollis, E.R. II, Jamshidi, P., Löw, K., Blesch, A. & Tuszynski, M.H. Induction of corticospinal regeneration by lentiviral *trkB*-induced Erk activation. *Proc. Natl. Acad. Sci. USA* **106**, 7215–7220 (2009).
- Xu, X.M., Guénard, V., Kleitman, N., Aebischer, P. & Bunge, M.B. A combination of BDNF and NT-3 promotes supraspinal axonal regeneration into Schwann cell grafts in adult rat thoracic spinal cord. *Exp. Neurol.* **134**, 261–272 (1995).
- Vavrek, R., Pearse, D.D. & Fouad, K. Neuronal populations capable of regeneration following a combined treatment in rats with spinal cord transection. *J. Neurotrauma* **24**, 1667–1673 (2007).
- Lu, P. *et al.* Motor axonal regeneration after partial and complete spinal cord transection. *J. Neurosci.* **32**, 8208–8218 (2012).
- Lee, Y.S. *et al.* Nerve regeneration restores supraspinal control of bladder function after complete spinal cord injury. *J. Neurosci.* **33**, 10591–10606 (2013).
- Cummings, B.J. *et al.* Human neural stem cells differentiate and promote locomotor recovery in spinal cord-injured mice. *Proc. Natl. Acad. Sci. USA* **102**, 14069–14074 (2005).
- Bonner, J.F. *et al.* Grafted neural progenitors integrate and restore synaptic connectivity across the injured spinal cord. *J. Neurosci.* **31**, 4675–4686 (2011).
- Lu, P. *et al.* Long-distance growth and connectivity of neural stem cells after severe spinal cord injury. *Cell* **150**, 1264–1273 (2012).
- Lu, P. *et al.* Long-distance axonal growth from human induced pluripotent stem cells after spinal cord injury. *Neuron* **83**, 789–796 (2014).

21. Peljto, M., Dasen, J.S., Mazzoni, E.O., Jessell, T.M. & Wichterle, H. Functional diversity of ESC-derived motor neuron subtypes revealed through intraspinal transplantation. *Cell Stem Cell* **7**, 355–366 (2010).
22. Ma, L. *et al.* Human embryonic stem cell–derived GABA neurons correct locomotion deficits in quinolinic acid-lesioned mice. *Cell Stem Cell* **10**, 455–464 (2012).
23. Mayer-Proschel, M., Kalyani, A.J., Mujtaba, T. & Rao, M.S. Isolation of lineage-restricted neuronal precursors from multipotent neuroepithelial stem cells. *Neuron* **19**, 773–785 (1997).
24. Du Beau, A. *et al.* Neurotransmitter phenotypes of descending systems in the rat lumbar spinal cord. *Neuroscience* **227**, 67–79 (2012).
25. Perry, R.B. *et al.* Subcellular knockout of importin β 1 perturbs axonal retrograde signaling. *Neuron* **75**, 294–305 (2012).
26. Cho, Y., Sloutsky, R., Naegle, K.M. & Cavalli, V. Injury-induced HDAC5 nuclear export is essential for axon regeneration. *Cell* **155**, 894–908 (2013).
27. Fawcett, J.W., Schwab, M.E., Montani, L., Brazda, N. & Müller, H.W. Defeating inhibition of regeneration by scar and myelin components. *Handb. Clin. Neurol.* **109**, 503–522 (2012).
28. Liu, Y. & Rao, M.S. Glial progenitors in the CNS and possible lineage relationships among them. *Biol. Cell* **96**, 279–290 (2004).
29. Cao, Q.L., Howard, R.M., Dennison, J.B. & Whittemore, S.R. Differentiation of engrafted neuronal-restricted precursor cells is inhibited in the traumatically injured spinal cord. *Exp. Neurol.* **177**, 349–359 (2002).
30. García-Alliás, G., Barkhuysen, S., Buckle, M. & Fawcett, J.W. Chondroitinase ABC treatment opens a window of opportunity for task-specific rehabilitation. *Nat. Neurosci.* **12**, 1145–1151 (2009).
31. Conner, J.M., Chiba, A.A. & Tuszynski, M.H. The basal forebrain cholinergic system is essential for cortical plasticity and functional recovery following brain injury. *Neuron* **46**, 173–179 (2005).
32. Montoya, C.P., Campbell-Hope, L.J., Pemberton, K.D. & Dunnett, S.B. The “staircase test”: a measure of independent forelimb reaching and grasping abilities in rats. *J. Neurosci. Methods* **36**, 219–228 (1991).
33. Wahl, A.S. *et al.* Neuronal repair. Asynchronous therapy restores motor control by rewiring of the rat corticospinal tract after stroke. *Science* **344**, 1250–1255 (2014).
34. Alaverdashvili, M. & Whishaw, I.Q. Motor cortex stroke impairs individual digit movement in skilled reaching by the rat. *Eur. J. Neurosci.* **28**, 311–322 (2008).
35. Whishaw, I.Q., Gorny, B. & Sarna, J. Paw and limb use in skilled and spontaneous reaching after pyramidal tract, red nucleus and combined lesions in the rat: behavioral and anatomical dissociations. *Behav. Brain Res.* **93**, 167–183 (1998).
36. Girgis, J. *et al.* Reaching training in rats with spinal cord injury promotes plasticity and task specific recovery. *Brain* **130**, 2993–3003 (2007).
37. Krajacic, A., Weishaupt, N., Girgis, J., Tetzlaff, W. & Fouad, K. Training-induced plasticity in rats with cervical spinal cord injury: effects and side effects. *Behav. Brain Res.* **214**, 323–331 (2010).
38. Steward, O., Sharp, K.G. & Matsudaira Yee, K. Long-distance migration and colonization of transplanted neural stem cells. *Cell* **156**, 385–387 (2014).
39. Tuszynski, M.H. *et al.* Neural stem cell dissemination after grafting to CNS injury sites. *Cell* **156**, 388–389 (2014).
40. Tuszynski, M.H. *et al.* Neural stem cells in models of spinal cord injury. *Exp. Neurol.* **261**, 494–500 (2014).
41. Steward, O., Sharp, K.G., Yee, K.M., Hatch, M.N. & Bonner, J.F. Characterization of ectopic colonies that form in widespread areas of the nervous system with neural stem cell transplants into the site of a severe spinal cord injury. *J. Neurosci.* **34**, 14013–14021 (2014).
42. Garcia-Ovejero, D. *et al.* The ependymal region of the adult human spinal cord differs from other species and shows ependymoma-like features. *Brain* **138**, 1583–1597 (2015).
43. Conti, L. & Cattaneo, E. Neural stem cell systems: physiological players or in vitro entities? *Nat. Rev. Neurosci.* **11**, 176–187 (2010).
44. Chen, H. *et al.* Human-derived neural progenitors functionally replace astrocytes in adult mice. *J. Clin. Invest.* **125**, 1033–1042 (2015).
45. Blackmore, M.G. *et al.* Krüppel-like Factor 7 engineered for transcriptional activation promotes axon regeneration in the adult corticospinal tract. *Proc. Natl. Acad. Sci. USA* **109**, 7517–7522 (2012).
46. Norenberg, M.D., Smith, J. & Marcillo, A. The pathology of human spinal cord injury: defining the problems. *J. Neurotrauma* **21**, 429–440 (2004).
47. Coumans, J.V. *et al.* Axonal regeneration and functional recovery after complete spinal cord transection in rats by delayed treatment with transplants and neurotrophins. *J. Neurosci.* **21**, 9334–9344 (2001).
48. Molofsky, A.V. *et al.* Astrocyte-encoded positional cues maintain sensorimotor circuit integrity. *Nature* **509**, 189–194 (2014).

ONLINE METHODS

Animals. A total of 248 rats were subjects of this study, including adult female Fischer 344 rats (150–200 g; $n = 224$; Harlan); embryonic male and female transgenic Fischer 344 rats expressing GFP ubiquitously (150–200 g; $n = 6$; Rat Resource and Research Center, University of Missouri, Columbia, Missouri); and athymic female nude rats (150–180 g; $n = 18$, T cell deficient; The Jackson Laboratory, Bar Harbor, Maine). A total of 41 mice were used in this study, including C57BL/6 female mice (25–35 g; $n = 31$; The Jackson Laboratory, Bar Harbor, Maine); transgenic embryonic male and female C57BL/6 GFP mice (25–35 g; $n = 10$; The Jackson Laboratory, Bar Harbor, Maine). US National Institutes of Health guidelines for laboratory animal care and safety were strictly followed. The Institutional Animal Care and Use Committee of the Department of Veterans Affairs (VA) San Diego Healthcare System approved all animal surgeries. Animals had free access to food and water throughout the study. All surgery was done under deep anesthesia using a combination (2 ml/kg) of ketamine (25 mg/ml), xylazine (1.3 g/ml) and acepromazine (0.25 mg/ml).

Cell preparation. All cells were prepared and grafted at a concentration of 200,000 cells per μl . Rat multipotent neural progenitor cells (NPCs) were prepared as described previously¹⁹. Briefly, E14 spinal cord anlage from F344 GFP-expressing transgenic rats was dissociated with 0.05% trypsin and re-suspended in phosphate-buffered saline (PBS). For T3 complete transection and C4 right-quadrant lesion models, E14-rat spinal cord–derived multipotent NPCs were suspended in a fibrin matrix (25 mg/ml fibrinogen and 25 U/ml thrombin, Sigma-Aldrich) containing a growth-factor cocktail to support graft survival, as previously described¹⁹. For grafts of rat NPCs in all other models, cells were re-suspended in PBS. For preparation of mouse multipotent NPCs, we used C57BL/6 mice expressing GFP under the ubiquitin promoter. E12-mouse spinal cords dissected and dissociated by using the methods described above. Mouse neuronal-restricted precursors (NRPs) and glial-restricted precursors (GRPs) were prepared as described previously⁴⁹ from E12-mouse GFP-expressing spinal cords. On the day of transplantation, cells were dissociated with Accutase (Innovative Cell Technologies, San Diego, California) and re-suspended in PBS. The human spinal cord neural progenitor cell line UCSD1113 was generated from a 9-week-old embryonic spinal cord that was dissociated and incubated with TrypLE (Life Technologies, Grand Island, New York) for 20 min, followed by light mechanical dissociation. Dissociated cells were cultured on plates coated with CELLstart, using KnockOut Dulbecco's Modified Eagle's Medium (DMEM) mixed with F12 culture medium, supplemented with 2% of StemPro Neural Supplement (all from Life Technologies, Grand Island, New York), 20 ng/ml, fibroblast growth factor 2, 20 ng/ml epidermal growth factor, 10 ng/ml leukemia inhibitory factor, 1% of Glutamax and 1% penicillin-streptomycin. Cells were expanded to passage 3, dissociated with Accutase and resuspended in a fibrin matrix containing the growth-factor cocktail. Human neural stem cells derived from the H9 ES cell line were purchased from Life Technologies (Grand Island, New York) and infected overnight with GFP-expressing lentivirus under the cytomegalovirus early enhancer chicken β actin (CAG) promoter. Greater than 97% of the cells expressed GFP *in vitro*. Human induced pluripotent stem cells (hiPSCs, line IMR90, donated from James Thompson lab at University of Wisconsin–Madison, passage 28–30) were maintained on a feeder layer of irradiated mouse embryonic fibroblasts (MEFs), as described^{50,51}. hiPSCs were differentiated to Pax6- and Sox1-expressing neuroepithelia (NE) for 10–12 d in a neural induction medium consisting of DMEM and F12, N2 supplement and nonessential amino acids⁵². The neuroepithelial cells formed neural tube–like rosettes at days 10–12, which were gently blown off by a 1-ml pipette on day 15. To generate forebrain NPCs, the spheres were suspended in the same medium. For generating spinal cord NPCs, RA (0.1 μM) was added every other day from days 10–23 to induce a spinal fate⁵³. Rat MSCs and primary cultured Schwann cells were prepared and grafted as described previously^{15,54,55}. Cell viability in all grafting experiments was assessed by trypan blue exclusion (Life Technologies, Grand Island, New York) at the conclusion of the grafting day, and was always within the range of 85–98%.

Spinal cord lesions. In this study, we used two lesion models for anatomical study: 1) T3 complete transection, a severe lesion that interrupts all axonal

projections across the lesion site; and 2) C4-CST lesions, which remove ~98% of corticospinal projections⁵ along with the majority of the dorsal column sensory projection and portions of surrounding gray matter and dorsolateral white matter; these lesions largely spare ventral white and gray matter. C4-CST lesions were used both to simplify animal care, and importantly, because this lesion allows graft-cell survival without the use of growth factors that might confound the experimental interpretation of mechanisms associated with CST regeneration². To make focal CST lesions, a tungsten wire knife was inserted 1 mm from the dorsal surface of spinal cord and raised 0.8 mm to transect the dorsal CST, leaving an overlying remnant of the dorsal column ascending sensory projection and thereby creating an enclosed lesion cavity with intact dura. T3 complete transections were employed to determine whether corticospinal axons are capable of regenerating in this most severe type of SCI, using previously described methods¹⁹. For behavior study, we used C4 right-quadrant lesions. To place C4 right-quadrant lesions, we performed bilateral dorsal column wire-knife lesions and right-dorsolateral wire-knife lesions: the wire knife was inserted into the right-dorsal aspect of the spinal cord, 0.5 mm from the midline. Facing medially, the knife was inserted to a depth of 1 mm, the arc of the knife was extruded and it was raised dorsally toward the spinal cord surface to transect the CST. The wire knife was then retracted and removed from the spinal cord, 180° to face toward the right lateral side of the spinal cord and re-inserted through the same opening to a depth of 1 mm. The blade was then extruded and raised again to the surface of the spinal cord. All animals within an experimental group that underwent lesions were randomly assigned to receive either neural grafts, non-neural grafts or lesion only.

Cell engraftment. In rats with T3 complete transections or C4 right-quadrant lesions, NPCs were grafted 2 weeks after the spinal cord lesion. 10 μl of cells (5 μl in the case of C4 quadrant lesions) were grafted into the lesion cavity through a pulled glass micropipette (OD 80 μm) using a PicoSpritzer II (General Valve, Inc., Fairfield, New Jersey). Subjects were perfused 6 weeks after grafting in T3-lesion subjects, and 13 weeks after grafting in C4 right-quadrant lesions.

For studies identifying mechanisms that enable rat corticospinal regeneration, 2.5 μl of rat NPCs were grafted into C4-CST injury sites immediately after lesions were placed. To study corticospinal axon bridging beyond the lesion, six adult Fisher 344 rats received 1.5 μl of neural progenitor cells, followed by perfusion 6 weeks later.

To determine whether corticospinal axonal regeneration requires an injury signal, C5-CST lesions were placed in adult Fischer 344 rats, and 1 μl of E14 rat spinal cord–derived NPCs were grafted into the dorsal column white matter at the C4 level. Cells were microinjected using an 80 μm –OD pulled glass micropipette at a depth of 0.5 mm from dorsal surface of spinal cord. Ten rats received C5 lesions and grafts of NPCs, and 11 rats received grafts alone without lesions. Any animals in which grafts were inadvertently placed within the corticospinal main tract at C4 were excluded from the analysis, because of the possibility that the graft itself caused an injury to the CST: accordingly, the final numbers of analyzed subjects was six per group.

To investigate whether corticospinal axonal regeneration requires physical contact with NPC grafts, ten subjects underwent C5-CST lesions and, on the same day, grafts of E14 rat spinal cord–derived NPCs at C4. These grafts were placed with the objective to just make contact with the CST at C4, or to be located slightly dorsally and not in actual physical contact. To be included in analysis, animals had to meet these proximity criteria, and grafts could not be located within the CST itself at C4. Out of the 15 animals implanted, six subjects were excluded because the graft was located within the corticospinal main tract, or because the graft distance from the tract was more than 50 μm . This left a total of nine subjects in which the graft just made contact with the graft ($n = 5$) or in which the graft was very close to, but not in contact with, the graft ($n = 4$).

To determine whether grafts of mature NPC grafts can support corticospinal regeneration, adult F344 rats underwent microinjections of E14 rat spinal cord–derived multipotent NPC grafts into intact, unlesioned C4 dorsal columns at a depth of 0.5 mm, aiming for contact with, but no lesion of, the corticospinal projection. C5-CST lesions were then placed either on the same day as grafting ($n = 9$), 20 d after grafting ($n = 8$) or 70 d after grafting ($n = 12$). Additional animals underwent identical grafts to the intact C4 dorsal columns with

maturation for 7 d ($n = 3$), 20 d ($n = 5$) or 70 d ($n = 5$), but C5 was never lesioned. In all animals, a total of 1 μ l of cells were injected into the intact C4 dorsal columns. Subjects in which NPCs were inadvertently injected directly with the CST were excluded from analysis, leaving $n = 5$ animals with grafts and lesions at the same time, $n = 4$ animals with grafts followed by lesions 20 d later and $n = 6$ animals with grafts and lesions 70 d later. Among animals that received grafts to the dorsal columns for 0, 20 or 70 d without C5 lesions, $n = 3$ per group per time point met graft placement requirements.

For studies examining whether neurons in grafts were required to enable corticospinal regeneration, C57BL/6 mice were used, and C4-CST lesions were placed. At the same time as injury, cells were grafted into the lesion site. Nine mice received grafts of glial-restricted precursors (GRPs), and four mice received a mixture of NRPs and GRPs. Nine additional mice received grafts of E12 mouse-derived, multipotent NPCs. Six weeks after grafting, all mice were perfused.

For human neural stem cell grafting studies, C4 corticospinal lesions were performed in adult immunodeficient rats. Two weeks later, 2.5- μ l suspensions of human multipotent NPCs from embryonic spinal cord ($n = 6$), human H9 ES cell line-derived neural stem cells ($n = 9$), rostralized hiPSC-derived neural stem cells ($n = 4$) or caudalized hiPSC-derived neural stem cells ($n = 4$) were injected into the lesion site, followed by perfusion 6 weeks later.

For anatomical MSCs or Schwann cell-transplantation studies, female adult Fisher rats underwent 2.5 μ l of cell-suspension graft of MSCs-GFP ($n = 6$), MSCs-NT3-GFP ($n = 6$), MSCs-BDNF-GFP ($n = 6$) or Schwann cells ($n = 6$) into C4-CST lesion at the same time of injury, followed by perfusion 6 weeks later.

Electrophysiology. To examine synaptic function between regenerating corticospinal axons and neural grafts, three rats received 16 injections of AAV2-CAG-CHR2-GFP (6 μ l; 1.0×10^{12} particles per ml, UNC Vector Core, Chapel Hill, North Carolina) into bilateral motor cortices at coordinates described previously⁵. Two weeks later, C4-CST lesions were placed, and NPCs were grafted into the lesion site. Four weeks later, animals were transcardially perfused for 3 min with ice-cold, oxygenated, modified sucrose artificial cerebrospinal fluid (ACSF) containing (in mM) 75 NaCl, 2.5 KCl, 3.3 MgSO₄, 0.5 CaCl₂, 1NaH₂PO₄, 26.2 NaHCO₃, 22 glucose, 52.6 sucrose, 10 4-(2-hydroxyethyl)-1-piperazineethanesulfonic acid (HEPES), 10 choline chloride, 1 pyruvate and 1 L-ascorbic acid (~300 mOsm; pH 7.4). A 1.5 cm-long section of the spinal cord containing the graft was rapidly dissected, and the dura was removed. The cord was mounted onto an agarose block, and sagittal slices (330 μ m) were cut and collected in ice-cold, oxygenated, modified sucrose ACSF. Slices were transferred to an interface chamber containing the same modified sucrose ACSF solution and incubated at 34 °C for 30 min. Slices were held at room temperature (23 °C) in the interface chamber for at least 45 min before recordings were initiated. Recordings were made in a submersion-type recording chamber and perfused with oxygenated ACSF containing (in mM) 119 NaCl, 2.5 KCl, 1.3 MgCl₂, 2.5 CaCl₂, 1.3 NaH₂PO₄, 26.0 NaHCO₃, 20 glucose (~300 mOsm) at 23 °C at a rate of 2–3 ml/min. RFP-expressing grafts were initially identified by their fluorescence emission spectra and were then targeted for whole-cell recording under infrared differential interference contrast videomicroscopy (Olympus BX-51 scope and Rolera XR digital camera). Whole-cell patch-clamp recordings were obtained with Multiclamp 700B patch amplifiers (Molecular Devices), and data were analyzed using pClamp 10 software (Molecular Devices). Voltage and current clamp recordings were made at room temperature by using pulled patch pipettes (4–7 M Ω) filled with internal solution containing (in mM) 150 K-gluconate, 1.5 MgCl₂, 5.0 HEPES, 1 ethylene glycol tetraacetic acid (EGTA), 10 phosphocreatine, 2.0 ATP and 0.3 GTP. To stimulate corticospinal axons, graft-containing slices were exposed to a 5 ms pulse of 470 nm light (delivered by a light-emitting diode (LED); Thor Labs), or extracellular bipolar electrodes (500- μ m interelectrode spacing) were placed in the CST 1 mm above the graft. Postsynaptic responses were analyzed exclusively from graft cells with a resting membrane potential ≤ -55 mV, with drift < 6 mV over the entire recording period, with access resistance ≤ 35 M Ω , and with the ability to evoke multiple spikes with > 60 mV peak amplitude from threshold.

Anterograde and retrograde tracing. To trace corticospinal axons in rats, 5 μ l of 10% BDA (MW 10,000, Life Technologies, Grand Island, New York) was injected into eight sites per hemisphere, into bilateral motor cortices

2 weeks before perfusion⁵. In mice, 2.5 μ l of BDA were injected into five sites per hemisphere⁸.

Retrograde labeling of graft neurons extending axons to caudal spinal cord segments was conducted by injecting 1 μ l CTB (1% solution; List Biological Laboratories, Campbell, California) into bilateral C6/7 spinal gray matter in four Fischer 344 rats that had undergone C4-CST lesions and grafts of NPCs into the lesion site. CTB was injected 6 weeks after lesion and grafting, and animals were perfused 3 d later.

Histology and immunohistochemistry. Spinal cords with T3 complete transections and grafts were horizontally sectioned on a cryostat at 30- μ m intervals. All other spinal cords containing the lesion and graft site were sagittally sectioned at 30- μ m intervals. Sections were incubated with primary antibodies against GFP (rabbit from Invitrogen at 1:1,000 or chicken from Abcam at 1:1,000); GFAP (mouse from Chemicon at 1:1,000 or rabbit from Dako at 1:750 to label astrocytes); human GFAP (rabbit from Origene at 1:500 to label human-specific astrocytes); NeuN (mouse from Chemicon at 1:500 to label mature neurons); ChAT (goat from Chemicon at 1:250 to label spinal cord motor neurons); MAP2 (mouse from Chemicon at 1:2,000 to label dendrites); VGLUT1 (mouse from Chemicon at 1:1,000 to label glutamatergic terminals); synaptophysin (mouse from Chemicon at 1:1,000 to label presynaptic terminals); APC (mouse from Oncogene at 1:400 to label oligodendrocytes); NG2 (rabbit from Millipore at 1:400 to label oligodendrocyte precursors); Hu (human at 1:1,000 to label neurons, generous gift from Robert Darnell, The Rockefeller University, New York); doublecortin (DCX, goat from Santa Cruz at 1:250 to label immature neurons); nestin (mouse from BD at 1:200 to label NPCs); neurofilament (NF200; mouse from Millipore at 1:250 to label axons); 27C7 (mouse at 1:200 to label Schwann cells, generous gift from K. Wewetzer, University of Freiburg, Freiburg, Germany); RFP (mouse from Abcam at 1:200); human nuclei (mouse from Merck Millipore at 1:200); PAX6 (rabbit from Covance at 1:1,000); PAX6 (mouse from DHSB at 1:5,000); SOX1 (Goat from R&B at 1:1000); HoxB4 (Rat from DHSB at 1:50); FOXG1 (rabbit from Abcam at 1:100); OTX2 (goat from R and D at 1:2,000); EN1 (mouse from DHSB at 1:800); CAMK2 (rabbit from Genetex at 1:200); and Dyelight 405 or 594-conjugated streptavidin (from Invitrogen at 1:250 to label BDA-traced CST axons). Then, sections were incubated in Alexa 488, 594, or 647 conjugated goat or donkey secondary antibodies (1:500, Invitrogen) for 2.5 h at room temperature. For nuclear staining, 4',6-diamidino-2-phenylindole (DAPI; 200 ng/ml) was added to the final wash. Electron-microscopy analysis of synapse formation was performed as published previously¹⁹.

Quantification of corticospinal axons. The number of corticospinal axons regenerating into grafts in lesion sites was quantified with StereoInvestigator (MicroBrightField, <http://www.mbfioscience.com>), as previously described^{4,19}. Briefly, one in six sections were stained for BDA-labeled CST axons. Dorsal-to-ventral virtual lines were placed at 100 \times magnification, and then examined under 400 \times magnification. BDA-labeled axons that intersected the line were marked and counted. In the T3 complete-transection model, all sections were used for quantification. In the C4 dorsal column-lesion model, two sagittal sections containing the heaviest density of corticospinal main tract axons were quantified by using the same methods. In some experiments, we also measured the density of corticospinal axons in grafts (Fig. 3 and Supplementary Fig. 3), as described previously⁴. By using the same method, we also quantified the density of the main CST itself, outside the graft, and calculated the density of corticospinal axons in the graft relative to the main tract. All measurements were performed with the examiner blinded to group identity.

Quantification of glial scars. Fluorescently immunolabeled sections for GFAP and GFP were used to quantify the percentage of the field occupied by GFAP immunoreactivity surrounding the graft-lesion cavity or lesion cavity alone, as previously described⁵⁶. A 100 μ m-wide zone surrounding the lesion site was quantified in this manner.

Quantification of cell types in grafts. To quantify neuronal differentiation in E14 rat-derived NPC grafts, fluorescently immunolabeled sections for NeuN, GFAP, APC, GFP and DAPI were used. By using confocal microscopy (Olympus FV-1000), a minimum of 500 cells per graft were sampled in images (600 \times magnification)

from randomly selected regions of grafts. The proportion of neural marker-expressing cells to total number of DAPI was then calculated and averaged among groups. For the quantification of neural differentiation in human cell grafts, Hu, human GFAP, NG2 and human nuclei were used. By using the same method described above, the proportion of neural marker-expressing cells to total human-cell number was calculated and averaged among groups.

Behavioral studies. Eighteen adult female Fischer rats were trained on the staircase task for 3 weeks before undergoing C4 right-quadrant lesions. The staircase task (Lafayette Instrument Company, Lafayette, Indiana) was performed as described previously⁵⁷. Briefly, rats were allowed 15 min to consume sugar pellets *ad libitum* while in the apparatus. Investigators blinded to group identity recorded the number of pellets displaced, eaten or dropped, and the deepest stair level reached. Pellet-retrieval accuracy was calculated as a percentage of sugar pellets displaced that were eaten. All subjects underwent weekly post-grafting functional testing until the end of the behavioral-testing period.

Quantitative reverse transcription-polymerase chain reaction (RT-PCR). Total RNA was isolated from NPC cultures using the RNeasy Mini kit (Qiagen, Germantown, Pennsylvania) by following the manufacturer's protocol. Human fetal whole-brain and spinal cord RNAs were purchased from Clontech (Mountain View, California) and used as controls. For complementary DNA synthesis, the reverse-transcription reaction was performed by using the PrimeScript RT Master Mix (Perfect Real Time, Clontech), and quantitative PCR was performed by using the primers listed in **Supplementary Table 1** and SYBR Premix Ex Taq II (Tli RNase H Plus, Clontech) in 20- μ L reactions. Data were normalized to glyceraldehyde-3-phosphate-dehydrogenase expression (GAPDH).

Statistical analysis. Multiple group comparisons were made by Kruskal-Wallis ANOVA with Steel-Dwass test (**Fig. 5b** and **Supplementary Figs. 3d,e, 7d** and **4b**) or repeated-measures ANOVA (**Fig. 5c**). Two-group comparison was made by using the Wilcoxon test (**Figs. 2i, 4g,j** and **Fig. 6b,d**). Normality of data was assessed using the Shapiro-Wilk test. All statistics were performed by JMP software (SAS, Cary, North Carolina) with a designated significance level of 95%. Data are presented as mean \pm s.e.m. As stated above, observers were blinded to group identity while performing all quantifications.

49. Wu, Y., Liu, Y., Chesnut, J.D. & Rao, M.S. Isolation of neural stem and precursor cells from rodent tissue. *Methods Mol. Biol.* **438**, 39–53 (2008).
50. Thomson, J.A. *et al.* Embryonic stem cell lines derived from human blastocysts. *Science* **282**, 1145–1147 (1998).
51. Yu, J. *et al.* Induced pluripotent stem cell lines derived from human somatic cells. *Science* **318**, 1917–1920 (2007).
52. Zhang, S.C., Wernig, M., Duncan, I.D., Brüstle, O. & Thomson, J.A. *In vitro* differentiation of transplantable neural precursors from human embryonic stem cells. *Nat. Biotechnol.* **19**, 1129–1133 (2001).
53. Hu, B.Y. & Zhang, S.C. Differentiation of spinal motor neurons from pluripotent human stem cells. *Nat. Protoc.* **4**, 1295–1304 (2009).
54. Weidner, N., Blesch, A., Grill, R.J. & Tuszynski, M.H. Nerve growth factor-hypersecreting Schwann cell grafts augment and guide spinal cord axonal growth and remyelinate central nervous system axons in a phenotypically appropriate manner that correlates with expression of L1. *J. Comp. Neurol.* **413**, 495–506 (1999).
55. Kadoya, K. *et al.* Combined intrinsic and extrinsic neuronal mechanisms facilitate bridging axonal regeneration one year after spinal cord injury. *Neuron* **64**, 165–172 (2009).
56. Jones, L.L. & Tuszynski, M.H. Spinal cord injury elicits expression of keratan sulfate proteoglycans by macrophages, reactive microglia, and oligodendrocyte progenitors. *J. Neurosci.* **22**, 4611–4624 (2002).
57. Wang, D., Ichiyama, R.M., Zhao, R., Andrews, M.R. & Fawcett, J.W. Chondroitinase combined with rehabilitation promotes recovery of forelimb function in rats with chronic spinal cord injury. *J. Neurosci.* **31**, 9332–9344 (2011).